Mechanism for thermoelectric figure-of-merit enhancement in regimented quantum dot superlattices

Alexander A. Balandin[a)] and Olga L. Lazarenkova
Department of Electrical Engineering, University of California-Riverside, Riverside, California 92521

(Received 9 September 2002; accepted 27 November 2002)

We propose a mechanism for enhancement of the thermoelectric figure-of-merit in regimented quantum dot superlattices. A proof-of-concept calculation has been carried out for *p*-type regimented superlattice of Ge dots on Si. It is shown that when conditions for miniband formations are satisfied, carrier transport in such structures can be tuned in a favorable way leading to large carrier mobility, Seebeck coefficient, and, as a result, to the thermoelectric figure-of-merit enhancement. To maximize the improvement, one has to tune the parameters of quantum dot superlattice in such a way that electrical current is mostly through the well-separated minibands of relatively large width (at least several $k_B T$, where k_B is Boltzmann's constant and T is temperature). © *2003 American Institute of Physics.* [DOI: 10.1063/1.1539905]

Quantum dot superlattices (QDS), e.g., multiple arrays of quantum dots, have recently been proposed for thermoelectric applications.[1–3] It was suggested that improvement in such structures should come from the decreased lattice thermal conductivity due to additional acoustic phonon scattering and quantum confinement of *carriers*. At the same time, a simplistic scenario of the process when carriers are confined inside the dots and electrical conduction is due to carrier hopping between the dots does not lead to improvement in thermoelectric properties. Indeed, hopping conductivity is characterized by very low mobility.[4] It is also unlikely that above-the-barrier transport due to thermal excitation or applied bias would significantly contribute to the current for any realistic thermoelectric device. The situations when the main current contribution comes from carrier transport through wetting layers fall to another category since in this case the structure is closer to conventional multiple quantum well (QW) structures which have been studied in detail.[5–7] Thus, in order to achieve improvement of thermoelectric properties in QDS beyond those offered by QWs one should not rely only on thermal conductivity decrease, but also envision new ways for optimizing the carrier transport. In this letter we argue that in order to achieve "electron transmitting-phonon blocking" regime one can use regimented QDS where carrier transport is facilitated by miniband formation.

In the following we consider three-dimensionally (3D) regimented QDS with strong coupling among the dots. QDS with 3D regimentation has already been reported.[8] Strong coupling and regimentation lead to formation of 3D extended minibands instead of localized quantum dot states.[9] Such energy spectrum modification is expected to take place provided that the dot size is homogeneous and the dots are crystalline with low surface defect concentration. Formation of extended electron states and minibands have also already been observed in self-assembled multiple quantum-dot arrays.[4,10] Our model predictions will be made under simplifying assumption of perfect regimentation of quantum dots in QDS. At the same time, our results can be extended to realistic QDS with some degree of disorder as long as the miniband width is larger than the total inhomogeneous broadening. A recent theoretical study based on a solution of the Daniel–Duke equation[11] for disordered QDS has shown that even large configurational disorder (about 1/8th of QD size) can be neglected, while morphological disorder leads to broadening of conductance peaks but does not completely destroy the minibands.

We calculate electron spectrum of QDS in the envelope wave function approximation applied to a potential barrier profile of choice. The Schrödinger equation is written as:

$$\left[-\frac{\hbar^2}{2}\nabla_r \frac{1}{m^*}\nabla_r + V(\mathbf{r})\right]\varphi(\mathbf{r}) = E\varphi(\mathbf{r}), \tag{1}$$

where $\hbar$ is Planck's constant, $1/m^*$ is the reciprocal effective mass tensor, E is the electron energy, and the confining potential profile $V(r)$ corresponds to an infinite sequence of quantum dots of size L_x, L_y, and L_z separated by the barriers of thickness H_x, H_y, and H_z. The profile $V(\mathbf{r})$ is set to zero in the barrier region, while inside quantum dot it is equal to the band offset. The effect of strain is taken into account by changing the value of the corresponding band offset. We solve this equation both using the finite difference method (FDM)[12] and using a semianalytical approach to calculate electron dispersion in QDS with a model confining potential that allows for electron wave function separation.[9] The good agreement of the results for the below-the-barrier states[12] validates further use of the simplified model for electron dispersion in carrier transport calculations.

As an example material system we consider Ge quantum dots grown on Si. Although state-of-the-art Ge/Si QDS are characterized only by partial regimentation, continuous progress in MBE will likely lead to synthesis of 3D regimented QDS similar to those in Ref. 8. We restrict our analysis to heavy holes in Ge/Si QDS. This is done for two reasons. First, most of the band-gap discontinuity between Si and Ge goes to the valence band. Second, we can use the single-valley effective mass approximation since a single potential energy maximum in the valence band is located in Γ point. In addition, our proof-of-concept calculations are fa-

[a)]Author to whom correspondence should be addressed; electronic mail: alexb@ee.ucr.edu

0003-6951/2003/82(3)/415/3/$20.00 © 2003 American Institute of Physics
Downloaded 23 Jan 2003 to 138.23.167.22. Redistribution subject to AIP license or copyright, see http://ojps.aip.org/aplo/aplcr.jsp

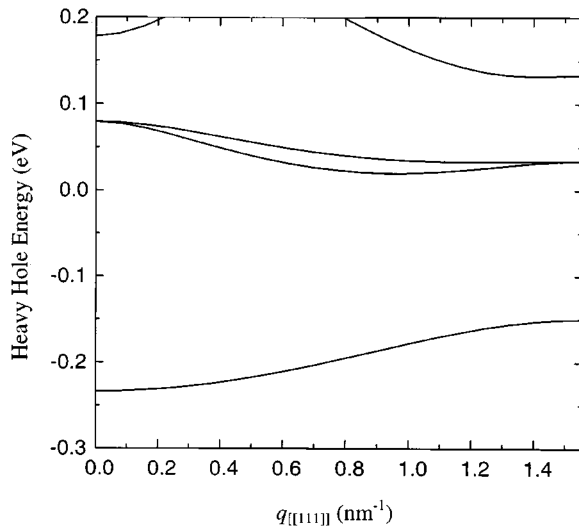

FIG. 1. Heavy-hole dispersion in tetragonal Ge/Si quantum dot superlattice with the following parameters: $L_x = L_y = 5$ nm, $L_z = 2.5$ nm, $H_x = H_y = 2.5$ nm, and $H_z = 1.25$ nm along ([111]) quasicrystallographic direction. The depth of potential well is $V = 450$ meV. The energy in units of eV is counted from the position of the potential barrier.

cilitated by the fact that the light-hole subband in compressed Ge is well separated from the heavy-hole subband and have much smaller effective mass, e.g., larger quantum confinement energies. The spin-orbit splitoff subband in Ge is omitted from consideration since even in relaxed bulk material it is separated from the heavy-hole subband with $E(\Gamma_{7v}) = -290$ meV energy gap and the minibands emanating from this subband do not contribute significantly to the mostly below-the-barrier miniband transport.

Figure 1 shows heavy-hole dispersion in Ge/Si QDS along ([111]) quasicrystallographic direction. Double brackets for the wave vector notation are introduced to distinguish direction in QDS from crystallographic directions. One can see the transformation of discrete levels of isolated quantum dots to minibands in 3D regimented quantum dot arrays. Similar to bulk crystals, the energy in QDS has the full symmetry of the reciprocal lattice. For example, the second miniband in Fig. 1, corresponding to the wave functions with one node per period in ([100]) or ([010]) quasicrystallographic direction and no nodes in other directions, is double degenerate in Γ and L points of the quasi-Brillouin zone. Far from the points of high symmetry in the center of QBZ and at its boundaries degeneracy due to wave function symmetry may be lifted. The width of minibands rapidly increases with shrinking of distance between quantum dots as we discussed in Ref. 9 and may be up to tens meV. The existence of the minibands means that holes can ''nearly freely'' move over the whole QDS structure instead of being confined in separate quantum dots. Their group velocity components strongly depend both on the miniband number and wave vector. It is interesting to note that in an ideal QDS, it is possible to achieve a very high carrier velocity (on the same order of magnitude as the thermal velocity in the host material). This fact is explained by the small size of the quasi-Brillouin zone in QDS as compared to the Brillouin zone in bulk crystals.

One can also notice from Fig. 1 that one-phonon assisted interminiband transitions can be suppressed for the considered structure. The latter is due to the formation of a complete minigap that depends on the width of the neighbor minibands in *every* direction. It follows from our calculations, that the separation between the first two minibands for given structure parameters is on the order of ~80 meV. Note that the maximum width of the first miniband in tetragonal QDS is along ([111]) direction, while that of the second miniband is along ([100]) and ([010]) quasicrystallographic directions. This minigap is larger than the energy of optical phonons in Si (64.3 meV) and Ge (37.2 meV). In order to further facilitate miniband transport, the width of the first minibands can be tuned up to $4k_BT$ by decreasing the QDS features size along chosen direction.

Based on the calculated carrier dispersion in QDS one can investigate the thermoelectric characteristics of this structure. The thermoelectric figure-of-merit is given as

$$ZT = \frac{\alpha^2 \sigma T}{\kappa}, \tag{2}$$

where α is the Seebeck coefficient, σ is the electrical conductivity, and $\kappa = \kappa_e + \kappa_L$ is thermal conductivity that includes electronic, κ_e, and phonon, κ_L contributions. We calculated all transport integrals necessary for evaluating ZT (Ref. 13) in constant relaxation time approximation[5] using semianalytical solution of Eq. (1) given in Ref. 9.

Figures 2(a) and 2(b) shows electrical conductivity and Seebeck coefficient α of QDS. The required transport coefficients were obtained by summation over all contributing minibands at the given temperature. The nonlinear behavior seen in Fig. 2(a) is explained by different number of minibands contributing to electric current as the Fermi level E_F shifts up in energy. The conductivity attains its minimum when E_F is in the gap between minibands. Since contributions of many minibands with different density of states are taken into account its position is not exactly in the middle of the gap. When carriers occupy about a half of the allowed states in miniband they can move nearly freely within this miniband over the whole QDS. This corresponds to quasimetallic conductivity of QDS characterized by rather large magnitude. It is known for bulk materials that α can be zero when electron and hole contributions exactly compensate each other. In the case of miniband transport $\alpha = 0$ when the contribution from carriers in the states with positive dispersion slope equal to that from the states with negative slope. Since one can switch the sign of Seebeck coefficient by shifting E_F, the QDS structure with the *p*-type doping but different doping density can be used for both legs of the thermoelectric device. One can also note that when E_F is far below the first miniband edge the QDS behavior is bulk-like.

The room temperature ZT as a function of the Fermi energy is plotted in Fig. 3. The curves show ZT for *p*-type Ge/Si QDS, which is normalized to the bulk Si ZT (see inset in Fig. 3) calculated using the same model and relaxation time value of 10^{-12} s. The lower curve is obtained under assumption that the phonon thermal conductivity of QDS is constant and equal to the bulk value in Si $\kappa_L = 156\ \mathrm{W\,m^{-1}\,K^{-1}}$. The upper curve is obtained under assumption that κ_L in QDS is decreased due to additional boundary scattering. Its value of $\kappa_L = 15\ \mathrm{W\,m^{-1}\,K^{-1}}$ was estimated from Ref. 3, where it has been calculated for similar Ge/Si QDS. For this estimation we used the volume frac-

Downloaded 23 Jan 2003 to 138.23.167.22. Redistribution subject to AIP license or copyright, see http://ojps.aip.org/aplo/aplcr.jsp

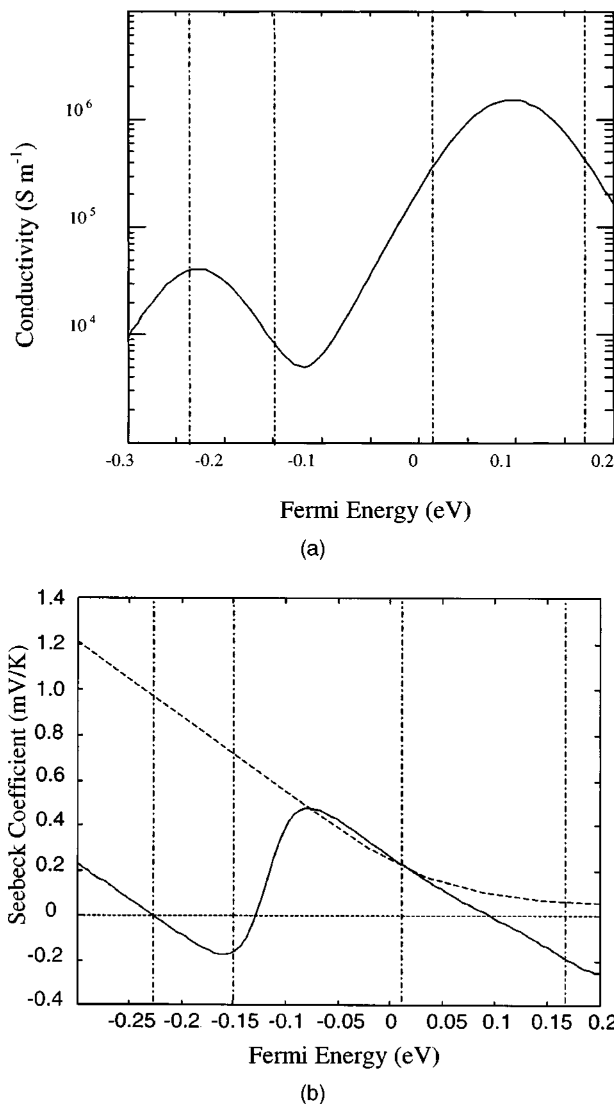

FIG. 2. (a) Electric conductivity at room temperature of *p*-type simple cubic regimented Ge/Si quantum dot superlattice as a function of Fermi energy. The structure is characterized by the following parameters: $L=2.5$ nm, $H=1.0$ nm, $V_e=0.45$ eV, $m_W^*=0.28\,m_0$, and $m_B^*=0.49\,m_0$. The depth of potential well is $V=450$ meV; (b) room temperature Seebeck coefficient for the quantum dot superlattice with the same parameters and bulk material (dashed line) as a function of Fermi energy. Vertical dot-dashed lines in both figures indicate miniband boundaries.

tion of Ge quantum dots in Si host to be $\delta=0.364$. As one can see there is a relatively large region of Fermi energies where *ZT* of QDS is one or two orders of magnitude larger than that of bulk Si. For comparison, the typical reported bulk Si *ZT* is 0.05 at 300 K.[14] Experimental value of bulk Si *ZT* at 323 K was found to be 0.01.[15] Abrikosov *et al.*[16] gave *p*-type $Si_{0.95}Ge_{0.05}$ *ZT* at 300 K as 0.06. Since accurate measurements of κ in QDS have not been carried out yet, at this moment it is not possible to select between the two curves shown in Fig. 3. A more rigorous theoretical treatment of κ would require finding acoustic phonon dispersion in such structures similar to those reported for quantum wells and nanowires.[17,18]

In conclusion, we proposed a structure and described a mechanism that can lead to significant *ZT* enhancement in regimented QDS. It has also been shown that by appropriate selection of Fermi level position one can switch a sign of the thermoelectric power in QDS. The predicted *ZT* enhancement together with an additional benefit of using the same type of QDS for both legs of thermoelectric device makes such structures very attractive as perspective materials for thermoelectric applications.

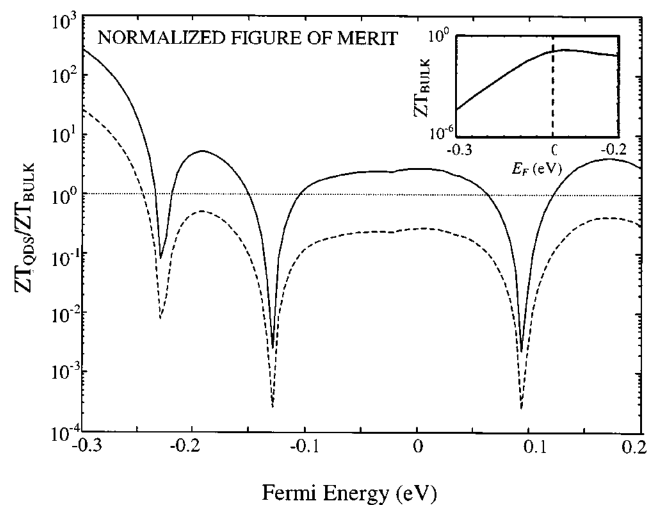

FIG. 3. Room temperature thermoelectric figure-of-merit *ZT* for *p*-type Ge/Si quantum dot superlattice normalized to the bulk Si value vs Fermi energy. Note an order of magnitude *ZT* increase in a wide range of QDS parameters over bulk silicon value. QDS parameters are the same as in Fig. 2. Solid line corresponds to $\kappa_L=15\ \mathrm{W\,m^{-1}\,K^{-1}}$, while dashed line corresponds bulk Si value of $\kappa_L=156\ \mathrm{W\,m^{-1}\,K^{-1}}$. The inset shows *ZT* for the bulk Si vs Fermi energy.

This work is supported in part by the NSF Nanoscale Exploratory Research (NER) Program on Quantum Dot Superlattices and CRDF-MRDA Project ME2-3010 on Low-Dimensional Thermoelectric Structures. The authors acknowledge useful discussions with Professor A. Casian, Professor K. L. Wang, Professor M. S. Dresselhaus, Professor G. Chen, Professor L. P. Pryadko, and Professor R. Lake.

[1] K. L. Wang and A. A. Balandin, in *Optics of Nanostructured Materials*, edited by V. Markel and T. George (Wiley, New York, 2001), p. 515.
[2] T. C. Harman, P. J. Taylor, D. L. Spears, and M. P. Walsh, J. Electron. Mater. **29**, L1 (2000).
[3] A. Khitun, A. A. Balandin, J. L. Liu, and K. L. Wang, J. Appl. Phys. **88**, 696 (2000).
[4] H. Z. Song, K. Akahane, S. Lan, H. Z. Xu, Y. Okada, and M. Kawabe, Phys. Rev. B **64**, 085303 (2001).
[5] L. D. Hicks, T. C. Harman, and M. S. Dresselhaus, Appl. Phys. Lett. **63**, 3230 (1993).
[6] H. Beyer, J. Nurnus, H. Bottner, A. Lambrecht, T. Roch, and G. Bauer, Appl. Phys. Lett. **80**, 1216 (2002).
[7] A. Casian, I. Sur, H. Scherrer, and Z. Dashevsky, Phys. Rev. B **61**, 15965 (2000).
[8] G. Springholz, M. Pinczolits, P. Mayer, V. Holy, G. Bauer, H. H. Kang, and L. Salamanca-Riba, Phys. Rev. Lett. **84**, 4669 (2000).
[9] O. L. Lazarenkova and A. A. Balandin, J. Appl. Phys. **89**, 5509 (2001).
[10] M. V. Artemyev, U. Woggon, H. Jaschinski, L. I. Gurinovich, and S. V. Gaponenko, J. Phys. Chem. **104**, 11617 (2000).
[11] I. Gomez, F. Dominguez-Adame, E. Diez, and P. Orellana, J. Appl. Phys. **92**, 4486 (2002).
[12] O. L. Lazarenkova and A. A. Balandin, Phys. Rev. B **66**, 245319 (2002).
[13] D. M. Rowe and C. M. Bhandari, *Modern Thermoelectrics* (Prentice-Hall, Englewood Cliffs, NY, 1983).
[14] C. N. Liao, C. Chen, and K. N. Tu, J. Appl. Phys. **86**, 3204 (1999).
[15] O. Yamashita and N. Sadatomi, J. Appl. Phys. **88**, 245 (2000).
[16] N. Kh. Abrikosov, V. S. Zemskov, E. K. Iordanishvili, A. V. Petrov, and V. V. Rozhdestvenskaya, Sov. Phys. Semicond. **2**, 1468 (1969).
[17] A. Balandin and K. L. Wang, Phys. Rev. B **58**, 1544 (1998); J. Appl. Phys. **84**, 6149 (1998).
[18] J. Zou and A. Balandin, J. Appl. Phys. **89**, 2932 (2001).

Downloaded 23 Jan 2003 to 138.23.167.22. Redistribution subject to AIP license or copyright, see http://ojps.aip.org/aplo/aplcr.jsp